The Journal of Immunology
RESEARCH ARTICLE | DECEMBER 15 2004

CXCR4-Tropic HIV-1 Envelope Glycoprotein Functions as a Viral Chemokine in Unstimulated Primary CD4+ T Lymphocytes[1] FREE

Karl Balabanian; ... et. al

J Immunol (2004) 173 (12): 7150–7160.
https://doi.org/10.4049/jimmunol.173.12.7150

CXCR4-Tropic HIV-1 Envelope Glycoprotein Functions as a Viral Chemokine in Unstimulated Primary CD4$^+$ T Lymphocytes[1]

Karl Balabanian,[2]* Julie Harriague,[2]* Christine Décrion,* Bernard Lagane,* Spencer Shorte,† Françoise Baleux,‡ Jean-Louis Virelizier,* Fernando Arenzana-Seisdedos,* and Lisa A. Chakrabarti[3]*

Interaction of HIV-1 envelope glycoprotein gp120 with the chemokine receptor CXCR4 triggers not only viral entry but also an array of signal transduction cascades. Whether gp120 induces an incomplete or aberrant set of signals, or whether it can function as a full CXCR4 agonist, remains unclear. We report that, in unstimulated human primary CD4$^+$ T cells, the spectrum of signaling responses induced by gp120 through CXCR4 paralleled that induced by the natural ligand stromal cell-derived factor 1/CXCL12. gp120 activated heterotrimeric G proteins and the major G protein-dependent pathways, including calcium mobilization, phosphoinositide-3 kinase, and Erk-1/2 MAPK activation. Interestingly, gp120 caused rapid actin cytoskeleton rearrangements and profuse membrane ruffling, as evidenced by dynamic confocal imaging. This coordinated set of events resulted in a bona fide chemotactic response. Inactivated HIV-1 virions that harbored conformationally intact envelope glycoproteins also caused actin polymerization and chemotaxis, while similar virions devoid of envelope glycoproteins did not. Thus gp120, in monomeric as well as oligomeric, virion-associated form, elicited a complex cellular response that mimicked the effects of a chemokine. HIV-1 has therefore the capacity to dysregulate the vast CD4$^+$ T cell population that expresses CXCR4. In addition, HIV-1 may exploit its chemotactic properties to retain potential target cells and locally perturb their cytoskeleton, thereby facilitating viral transmission. *The Journal of Immunology,* **2004, 173: 7150–7160.**

Entry of HIV-1 into target cells requires the sequential interaction of the surface envelope glycoprotein gp120 with the primary receptor CD4 and with the coreceptors CXCR4 or CCR5 (1–3). HIV-1 receptor and coreceptors play key roles in leukocyte signaling, which is relevant to the understanding of AIDS pathogenesis. Binding of gp120 to CD4 generates signals that perturb CD4 costimulatory function in Ag-specific responses and may lead to T cell anergy and apoptosis (4–7). Similarly, interaction of gp120 with the chemokine receptors CXCR4 or CCR5 activates an array of signal transduction pathways that may contribute to the immune dysfunction characteristic of HIV-1 infection (reviewed in Refs. 8 and 9). By exploiting the chemokine system, HIV-1 has the potential to perturb the migratory patterns and activation status of leukocytes. Importantly, generalized immune activation is also a hallmark of HIV-1 infection and is actually thought to drive the process of chronic CD4$^+$ T cell destruction (10–12).

Chemokine responses are mediated by chemoreceptors coupled to heterotrimeric G proteins and are characterized by the coordinated activation of phospholipase C, PI3K, and MAPK pathways (13–15). Chemoattractant gradients induce the polarization of the phosphoinositide signal transduction machinery, resulting in reorganization of the actin cytoskeleton and ultimately in directed cell migration (16). Triggering of chemoreceptors by HIV-1 envelope glycoprotein was shown to induce some, though often not all, of these responses, depending on the chemoreceptor used and of the nature of target cells (17–29). Previous studies showed that binding of gp120 from CXCR4-tropic (X4) HIV-1 strains to activated CD4$^+$ T cells induced the phosphorylation of kinases involved in cell adhesion and directed migration, such as Pyk-2 and PI3K (17, 18). The Erk-1/2 MAPK pathway was also activated by X4 gp120, though only in cells prestimulated through the TCR (19–21). In contrast, the natural ligand of CXCR4, the chemokine stromal cell-derived factor 1 (SDF-1)[4] (CXCL12), induced the Erk-1/2 pathway in both stimulated and unstimulated CD4$^+$ T cells (30). Other studies in activated T cells or macrophages showed a defective or limited capacity of gp120 from X4 strains to induce calcium flux and chemotactic responses as compared with gp120 from CCR5-tropic (R5) strains, raising the possibility that gp120 induced an incomplete or aberrant set of signals through CXCR4 (22–24, 31).

CXCR4 is expressed in most T cells to some degree, while CCR5 expression is restricted to activated and memory T cells (32). The emergence of X4 strains in late-stage infection is associated with an increased rate of CD4$^+$ T cell depletion and a poor prognosis (33). Although an expanded range of target cells may contribute to disease progression, the mechanism of CD4$^+$ T cell depletion by X4 strains is not entirely understood. In particular, it

*Viral Immunology Unit, †Platform for Dynamic Imaging, and ‡Organic Chemistry Unit, Pasteur Institute, Paris, France

Received for publication July 30, 2004. Accepted for publication September 27, 2004.

The costs of publication of this article were defrayed in part by the payment of page charges. This article must therefore be hereby marked *advertisement* in accordance with 18 U.S.C. Section 1734 solely to indicate this fact.

[1] This study was supported by the Agence Nationale de Recherches sur le SIDA (to K.B.), Sidaction (to J.H. and B.L.), and the SESAME program from Région Ile-de-France (to S.S.).

[2] K.B. and J.H. contributed equally to this work.

[3] Address correspondence and reprint requests to Dr. Lisa A. Chakrabarti, Unité d'Immunologie Virale, Institut Pasteur, 28 rue du Dr. Roux, 75724 Paris Cedex 15, France. E-mail address: chakra@pasteur.fr

[4] Abbreviations used in this paper: SDF-1, stromal cell-derived factor 1; PFA, paraformaldehyde; PTX, *Bordetella pertussis* toxin; MFI, mean fluorescence intensity; PH, pleckstrin homology; AT-2, aldrithiol-2.

0022-1767/04/$02.00

remains unclear how HIV-1 succeeds in depleting all $CD4^+$ T cell compartments, while infecting predominantly the activated $CD4^+$ T cell subpopulation (10, 11). The capacity of X4 envelope glycoproteins to signal through the ubiquitous CXCR4 receptor may contribute to $CD4^+$ T cell dysregulation even in the absence of productive infection. However, gp120-induced signaling is poorly characterized in the unstimulated $CD4^+$ T cell population, because most studies evaluated signaling in activated T cells or transformed T cell lines. Whether gp120-dependent signals can perturb the vast majority of primary $CD4^+$ T cells thus remains to be determined.

To address this issue, we set to systematically compare the signaling properties of gp120 and SDF-1 in unstimulated primary $CD4^+$ T cells. We report that the spectrum of signals induced by gp120 through CXCR4 paralleled that induced by SDF-1. We provide evidence that gp120 can directly activate heterotrimeric G proteins, a hallmark of chemokine responses. Of importance, gp120 triggered rapid rearrangements of the actin cytoskeleton, profuse membrane ruffling, and chemotaxis. Therefore, gp120 has the capacity to mimic the action of a chemokine on unstimulated primary $CD4^+$ T cells, a property that may underlie the generalized immune activation characteristic of late-stage HIV-1 infection.

Materials and Methods

Abs and reagents

Immunostainings were performed using FITC-conjugated anti-human CD4-V4 (clone L120) and PE-conjugated anti-human CXCR4 (clone 12G5) mAbs (BD Biosciences, San Jose, CA). Anti-phospho-p44/p42 MAPK (Thr^{202}/Tyr^{204}, clone E10) mAb, anti-p44/p42 MAPK, anti-Akt and anti-phospho-Akt (Ser^{473}) rabbit sera were purchased from Cell Signaling Technology (Beverly, MA). Peroxidase-conjugated anti-mouse and anti-rabbit secondary Abs were obtained from Amersham Biosciences Europe (Upsala, Sweden) and Vector Laboratories (Burlingame, CA), respectively. SDF-1 was synthesized as described (34). Recombinant HIV-1 LAI envelope glycoprotein (Env) gp120 subunit and recombinant soluble human CD4 (sCD4) were produced in a mammalian cell expression system, ensuring proper glycosylation and folding of the proteins (Progenics, Tarrytown, NY). Unless specified, SDF-1 and gp120 were used at 30 and 200 nM, respectively. The sCD4/gp120 complexes were generated by incubating sCD4 and gp120 at a 2.5:1 ratio. The bicyclam AMD3100 (AnorMED, Langley, Canada) and the *Bordetella pertussis* toxin (PTX; Calbiochem, San Diego, CA) were used at a final concentration of 1 μM and 1 μg/ml, respectively. The preparation of aldritiol-2-inactivated HIV-1 NL4–3 viral particles (AT-2 HIV-1) was performed as described, except that viruses were produced over a single cycle by calcium phosphate transfection of HEK 293-T cells (35, 36). The control preparation HIV-1 Δenv consisted in particles produced from an env-deleted NL4–3 provirus and processed exactly as the wild-type HIV-1 particles.

Isolation of primary $CD4^+$ T lymphocytes

Donors of leukocytes consisted in healthy volunteers referred at the Etablissement Français du Sang (Paris, France). PBMC were separated from fresh blood samples using a Ficoll-Paque Plus (Amersham Biosciences) density gradient centrifugation and negatively enriched for $CD4^+$ T cells by magnetic cell sorting following the manufacturer instructions (Miltenyi Biotec, Auburn, CA). Isolated cells were routinely >95% pure. We checked by cytofluorometry that $CD4^+$ T cells expressed high levels of membrane CXCR4 after the Ficoll procedure (mean fluorescence intensity (MFI) >300), as evaluated with the CellQuest software on a FACSCalibur flow cytometer (BD Biosciences). Primary $CD4^+$ T lymphocytes were cultured overnight in complete medium, consisting in RPMI 1640 medium supplemented with 10% heat-inactivated FCS, 10 mM HEPES, penicillin (100 U/ml), and streptomycin (100 μg/ml), before use in functional assays. Overnight culture in the absence of stimulation did not significantly change CXCR4 expression levels.

Membrane preparation and [^{35}S]GTPγS binding assay

Membrane preparations were obtained from 3×10^8 PBMC as described (37). PBMC were incubated for 30 min at 4°C in buffer A (15 mM Tris-HCl pH 7.5, 2 mM $MgCl_2$, 0.3 mM EDTA, 1 mM EGTA) and homogenized in a Dounce potter. After centrifugation (5 min at 500 $\times$ *g*), the supernatants were recovered and centrifuged at 40,000 $\times$ *g* for 30 min at 4°C. The pellets were resuspended in buffer A and centrifuged at 40,000 $\times$ *g* for 30 min. The final membrane pellets were resuspended in buffer B (75 mM Tris-HCl pH 7.5, 12.5 mM $MgCl_2$, 0.3 mM EDTA, 1 mM EGTA, 250 mM sucrose). The measurement of [^{35}S]GTPγS binding to crude membrane preparations was performed in 96-well microplates (NEN basic flashplates). Membranes (7 μg of proteins/well) were incubated for 15 min at 30°C in 20 mM HEPES containing 100 mM NaCl, 10 μg/ml saponin, 3 mM $MgCl_2$, and 1 μM GDP, in the presence or absence (basal [^{35}S]GTPγS binding) of appropriate ligands and/or inhibitors. Then 0.1 nM [^{35}S]GTPγS (Amersham Biosciences) was added to membranes, which were incubated for 30 min at 30°C. Microplates were counted for 2 min per well in a Wallac 1450 Microbeta Trilux counter (PerkinElmer Life Sciences, Boston, MA).

Evaluation of CXCR4 functions

For calcium mobilization assays, $CD4^+$ T lymphocytes (2×10^6) were loaded for 30 min at 37°C with 1 μM Indo-1/AM (Molecular Probes, Eugene, OR) in HBSS buffer containing 1 mM $CaCl_2$, 1 mM $MgCl_2$, and 1% FCS (38). After a wash, cells were resuspended in HBSS buffer and incubated at 37°C for 5 min before SDF-1 or gp120 stimulation. Indo-1 fluorescence was collected on a LSR flow cytometer (BD Biosciences) with the following configuration: UV excitation at 325 nm, emission at 405/20 nm and 500/11 nm for bound and free probe, respectively.

To assess the phosphorylation of Erk-1/2 MAPK, $CD4^+$ T lymphocytes (1×10^7 cells/ml) were serum-starved for 4 h before stimulation with SDF-1 or gp120 for 2 min. Reaction was stopped by adding ice-cold paraformaldehyde (PFA) to a final concentration of 1% and incubation on ice. Cells were permeabilized with ice-cold methanol and processed for intracellular staining as described (39), using the anti-phospho Erk-1/2 MAPK mAb, followed by the secondary Ab anti-mouse IgG1 conjugated to Alexa-488 (Molecular Probes). The percentage of phospho-Erk-1/2-positive cells was evaluated by flow cytometry. The same primary Ab was used in immunoblot experiments, using a reported protocol (40).

Actin polymerization was evaluated on $CD4^+$ T cells as described (41). Briefly, cells were incubated at 1×10^7 cells/ml in RPMI 1640 medium containing 20 mM HEPES in the presence or absence of appropriate inhibitors. SDF-1, gp120, or AT-2 HIV-1 was then added to the cell suspension. At each indicated time point (15 s to 5 min), a 50-μl aliquot was taken from the cell suspension and mixed with 200 μl of labeling buffer, consisting in 10^{-7} M FITC-phalloidin (Sigma-Aldrich, St. Louis, MO), 0.125 mg/ml L-α-phosphatidylcholine palmitoyl (Sigma-Aldrich), and 4.5% PFA in PBS. The kinetics of actin polymerization following one or two consecutive stimulations was monitored by flow cytometry. Results are expressed as follows: [(MFI after addition of ligand)/(MFI before addition of ligand)] $\times$ 100. MFI values assessed before addition of ligand were arbitrarily set at 100%.

Chemotaxis of $CD4^+$ T cells was evaluated using the Transwell system as described (42). The fraction of transmigrated cells was calculated as follows: [(number of cells migrating to the lower chamber)/(number of cells added to the upper chamber at the start of the assay)] $\times$ 100.

Statistical analyzes consisted in unpaired two-tailed *t* tests and were conducted with the Prism software (Graphpad).

Fluorescence imaging

The GFP-Akt-PH construct was kindly given by T. Meyer (43), and the GFP-actin was obtained from Clontech (San Jose, CA). $CD4^+$ T cells were transfected using the amaxa Nucleofector technology (Köln, Germany) and used 18 h after nucleoporation. Transfection rates >50% were routinely obtained as evaluated by flow cytometry. A total of 3×10^5 cells were plated in complete medium onto poly-lysine-coated glass coverslips for 1 h at 37°C, stimulated with 30 nM SDF-1 or 200 nM gp120, and fixed in PBS-4% PFA.

For polymerized actin staining, $CD4^+$ T cells were stimulated as above, fixed, and permeabilized in PBS-0.1% Triton X-100 for 10 min. Cells were then labeled with TRITC-phalloidin (Sigma-Aldrich) for 30 min, washed, and mounted in Vectashield medium containing DAPI (Vector Laboratories). Fluorescence was imaged on Zeiss microscopes (Oberkochen, Germany) using a Plan Apochromat $\times$63/1.4 oil immersion objective. Images were collected with a cooled CCD camera (CoolSNAP-HQ, Roper Scientific, Evry, France) piloted by MetaMorph imaging software (Universal Imaging, West Chester, PA) or with an Axiocam MRm camera and the AxioVision software (Zeiss). Optical sectioning was performed according to the "structured illumination" principle (44) using the ApoTome system (Zeiss). For time-lapse confocal imaging, images were collected with an Ultra*VIEW* RS spinning-disk system (PerkinElmer Life Sciences).

Quantitation of membrane fluorescence was performed on 12-bit images with the MetaMorph software by making regions inside and outside the cell, bordering the plasma membrane (45). The percentage of membrane fluorescence was computed as the ratio between the integrated fluorescence intensities at the membrane and in the whole cell. A quantitative analysis of cell deformation was obtained by computing the shape index [=(perimeter)^2/4π(surface)] (46). These values were computed from a semiautomatic definition of the outline of the cell with the MetaMorph software. When the cell is round, the shape index =1. Any deviation from a circle gives a shape index >1.

Results

gp120 activates heterotrimeric G proteins and induces calcium mobilization

We set to analyze the early signaling events induced upon binding of gp120 to CXCR4. Experiments were conducted with primary cells that were not preactivated in vitro to better model in vivo conditions. Activation of heterotrimeric G proteins was evaluated by measuring the binding of [^{35}S]GTPγS to membranes. The binding of this nonhydrolizable GTP analog reflects the amount of Gα proteins activated upon agonist addition. PBMC membranes pulsed with SDF-1 (30 nM) showed an increase in [^{35}S]GTPγS binding, which was abrogated in the presence of the CXCR4 antagonist AMD3100 (Fig. 1*A*). Experiments with gp120 were conducted at 200 nM, a concentration close to its reported K_d for CXCR4 (200–500 nM) (47, 48), to achieve significant occupancy of the receptor. PBMC membranes pulsed with gp120 showed an increase in [^{35}S]GTPγS binding, though the response was lower than that induced by SDF-1. gp120-induced signal was abrogated by AMD3100 treatment, indicating that gp120 activated heterotrimeric G proteins through its interaction with CXCR4.

Calcium mobilization was evaluated by the shift in fluorescence emission of the indicator Indo-1/AM. A pulse of SDF-1 caused calcium mobilization in primary CD4$^+$ T cells (Fig. 1*B*, *left*). The kinetics of the response was typical of chemokines, with a rapid and transient increase in cytoplasmic Ca^{2+} concentration. The viral ligand gp120 also caused calcium mobilization, with similar kinetics (Fig. 1*B*, *right*). Thus, gp120 induced heterotrimeric G protein activation and rapid calcium mobilization, two hallmarks of chemokine responses.

gp120 activates Erk-1/2 MAPK in primary CD4$^+$ T cells

To further delineate transduction pathways activated by gp120, we assessed the phosphorylation of the Erk-1/2 MAPK by cytofluorometry. Primary CD4$^+$ T cells stimulated with SDF-1 showed an activation of Erk-1/2, with half of the cells showing a shift in fluorescence of ~1 log (Fig. 2*A*). A pulse of gp120 at 200 nM also induced MAPK activation, with up to 40% cells positive for phospho-Erk-1/2. Pretreatment of CD4$^+$ T cells with AMD3100 abrogated MAPK activation in response to both SDF-1 and gp120, indicating that these signals were CXCR4-dependent. Immunoblot analysis showed that both Erk-1 and Erk-2 were phosphorylated, because two bands of expected molecular mass (44 and 42 kDa, respectively) were detected in stimulated samples (Fig. 2*B*). The specificity of the response was further confirmed by inhibition with PD98059, a specific inhibitor of the MAPK kinase MEK1, which controls Erk-1/2 activation (not shown). We next investigated the role of CD4 in MAPK responses to gp120. Preincubation of gp120 with an excess of sCD4 did not decrease the percentage of phospho-Erk-1/2-positive cells (Fig. 2*C*). Because the excess sCD4 prevented interaction of gp120 with cellular CD4, this finding indicated that signals through CD4 were not necessary for MAPK activation. The facilitating effect of sCD4 on MAPK responses likely resulted from sCD4-induced conformational changes in gp120, which are known to expose the coreceptor binding site (49, 50) and thus promote direct interaction with CXCR4.

Several groups reported that gp120 tested at concentrations lower or equal to 80 nM did not activate Erk-1/2 through CXCR4 (19–21). Because these concentrations were lower than the reported K_d of gp120 for CXCR4 (200–500 nM) (47, 48), we evaluated whether they were limiting for MAPK responses. Comparing Erk-1/2 phosphorylation at 80 and 200 nM gp120 revealed a threshold effect, with only one of six donors responding at 80 nM, vs five of six donors responding at 200 nM (Fig. 2*D*). The extent of MAPK activation induced by gp120 at 200 nM varied according to the donor and remained more heterogeneous than that induced by SDF-1, but was significantly higher than that seen with gp120 at 80 nM ($p = 0.04$). Thus, gp120 induced a dose-dependent activation of the Erk-1/2 MAPK pathway in unstimulated primary CD4$^+$ T cells.

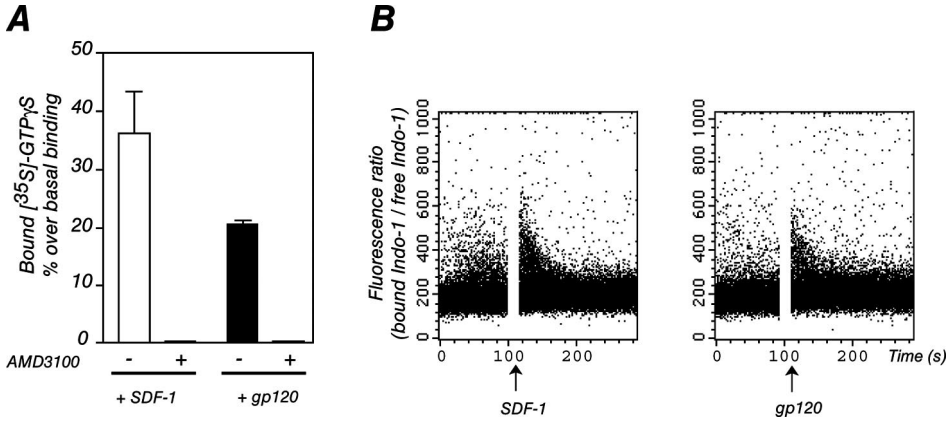

FIGURE 1. gp120 induces CXCR4-dependent G-protein activation in primary cells. *A*, For [^{35}S]GTPγS binding assays, PBMC membranes were incubated in buffer containing 0.1 nM [^{35}S]GTPγS in the presence or absence of SDF-1 or gp120, with or without AMD3100. Values are expressed as the percentage of bound [^{35}S]GTPγS over basal binding to membranes from PBMC cultured in the absence of ligands. Results indicate means ± SD from duplicate determinations and are representative of two independent experiments. *B*, To measure calcium flux, primary CD4$^+$ T lymphocytes were loaded with Indo-1/AM, and fluorescence intensity ratio at 405 nm/500 nm was analyzed by flow cytometry following stimulation (↑) with SDF-1 (*left*) or gp120 (*right*). Negative and positive controls, consisting in pulses with HBSS and the calcium ionophore ionomycin, respectively, were included in each experiment (not shown). Results are representative of three independent experiments.

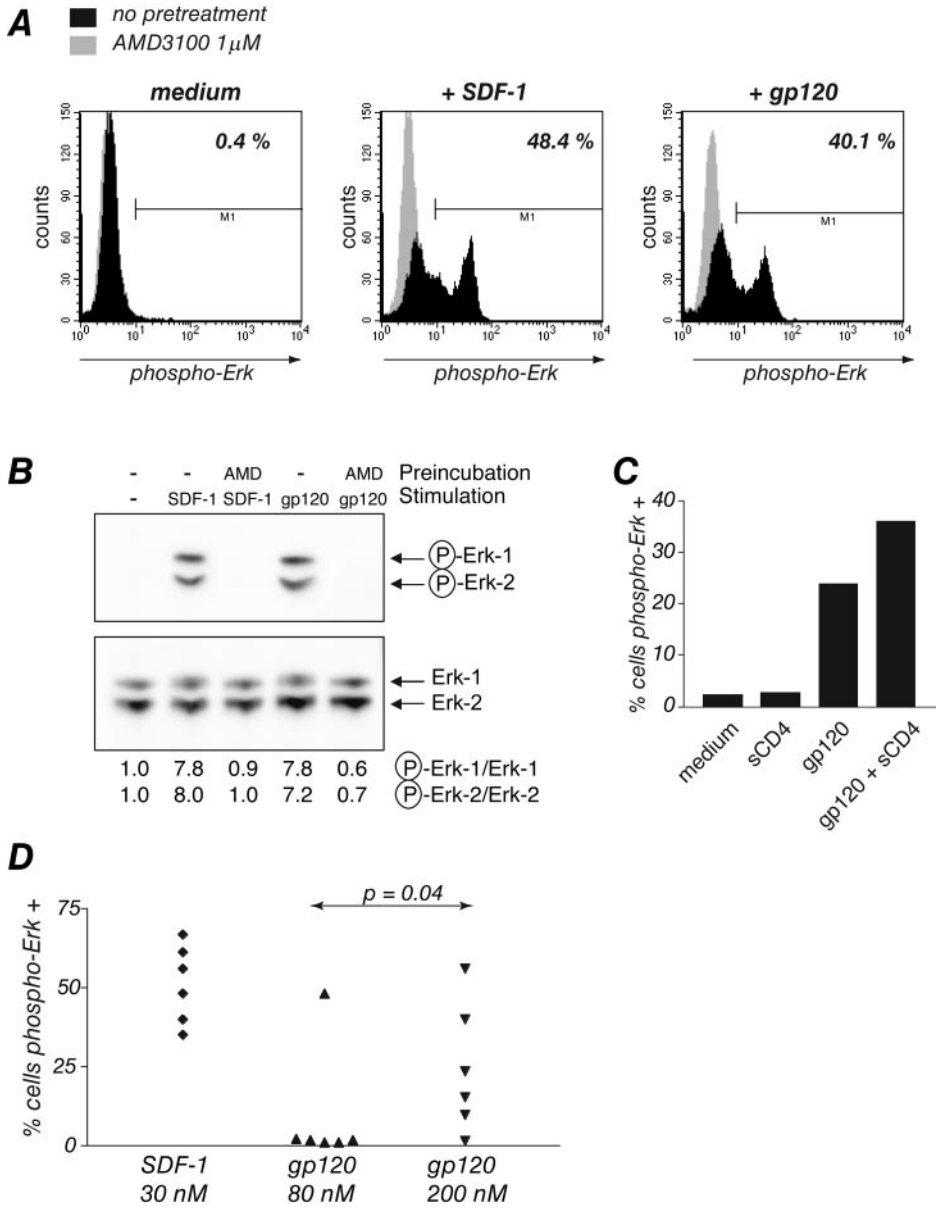

FIGURE 2. gp120 induces MAPK phosphorylation in primary $CD4^+$ T lymphocytes. *A*, For cytofluorometric detection of phosphorylated Erk-1/2, $CD4^+$ T cells, preincubated in the presence or absence of AMD3100 for 60 min, were stimulated for 2 min with SDF-1 or gp120. Phospho-Erk-1/2 content was analyzed by intracellular staining with a phospho-specific mAb. Histograms are shown for a representative donor. Gray histograms corresponds to samples pretreated with AMD3100. *B*, For detection of phospho-Erk-1/2 by immunoblot, protein extracts obtained from $CD4^+$ T cells treated as in *A* were separated by SDS-PAGE and probed with the anti-phospho-Erk-1/2 mAb (*upper panel*) or anti-Erk-1/2 Ab (*lower panel*). Quantitation of the phospho-Erk:total Erk ratio was done using a LAS-1000 CCD camera with the Image Gauge 3.4 software (Fuji Photo Film Co). The ratio was arbitrarily set at 1 for unstimulated cells. Results are representative of two independent experiments. *C*, $CD4^+$ T cells were treated with 500 nM sCD4, 200 nM gp120, or sCD4/gp120 complexes. Results are expressed as the percentage of cells positive for phospho-Erk-1/2 by cytofluorometry and are representative of three independent experiments. *D*, The percentage of phospho-Erk-1/2-positive cells was measured in response to different gp120 concentrations for six independent cell donors.

gp120 induces the PI3K pathway

We next evaluated the activation of the kinase Akt, which depends on PI3K activity. Upon activation, the pleckstrin homology (PH) domain of Akt binds with high affinity to the 3′-phosphoinositides generated by PI3K, which results in recruitment of Akt to the plasma membrane (45). Akt relocalization was monitored by following the distribution of the GFP-Akt-PH fusion protein by fluorescence microscopy. Primary $CD4^+$ T lymphocytes nucleoporated with the GFP-Akt-PH construct showed a diffuse distribution of the fluorescent probe in absence of CXCR4 ligands (Fig. 3*A*). Stimulation with gp120 or SDF-1 caused a rapid relocalization of GFP-Akt-PH to the plasma membrane, as evidenced by the increase in fluorescence at the cell periphery (Fig. 3*A*). In addition, morphological changes were observed in a fraction of the nucleoporated cells (~30%). Quantitation of fluorescent signal at the plasma membrane showed that both SDF-1 and gp120 caused a significant increase in GFP-Akt-PH membrane association (Fig. 3*B*). The relocalization induced by gp120 was slightly higher than that induced by SDF-1, which emphasized the potent effect of the viral ligand on the PI3K pathway.

The 3′-phosphoinositides generated by PI3K activity have a dual role in Akt activation. In addition to targeting Akt to the plasma membrane, they also activate the 3′-phosphoinositide-dependent kinase 1/2 kinases, which in turn phosphorylate Akt and make it enzymatically active. To further assess the activation status of Akt, we used an Ab that specifically detects the form of Akt phosphorylated at Ser^{473}. Immunoblot analysis showed that both SDF-1 and gp120 stimulation induced Akt phosphorylation (Fig. 3*C*). This event was CXCR4-dependent, as shown by inhibition by AMD3100 pretreatment. Thus, CXCR4 ligands induced both the relocalization and phosphorylation of Akt, resulting in full activation of the protein.

gp120 triggers rapid rearrangements of the actin cytoskeleton and promotes $CD4^+$ T cell chemotaxis

We next investigated the effects of gp120 on actin cytoskeleton rearrangements, which underlie cell polarization and motility. Actin polymerization was monitored by flow cytometry using the FITC-phalloidin probe as an indicator of F-actin content. Stimulation of primary $CD4^+$ T cells with SDF-1 caused a

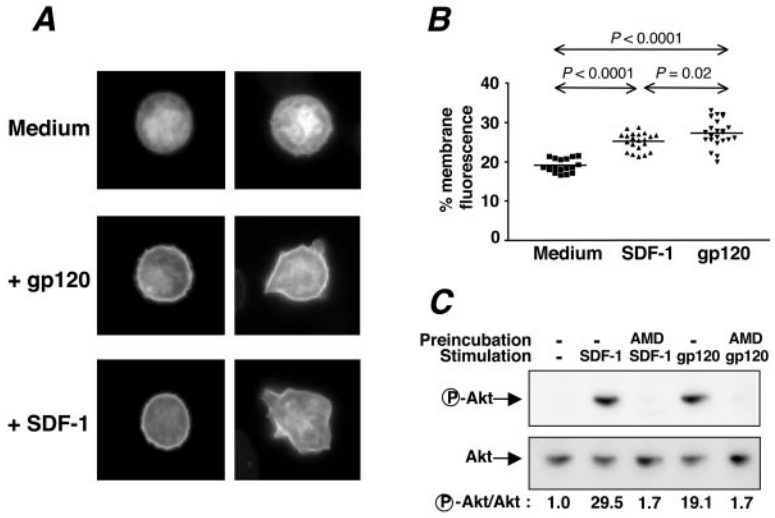

FIGURE 3. gp120 activates the PI3K pathway in primary $CD4^+$ T lymphocytes. *A*, The distribution of GFP-Akt-PH in $CD4^+$ T cells stimulated or not with SDF-1 or gp120 for 1 min was analyzed by fluorescence microscopy. Epifluorescence images of GFP-Akt-PH are shown in two representative cells after stimulation with medium, SDF-1, or gp120. *B*, Quantitative analysis of Akt redistribution (percentage of fluorescence at the membrane relative to total fluorescence) in $CD4^+$ T cells stimulated with SDF-1 or gp120. Lines show mean values. Data are representative of three independent experiments with >15 cells analyzed for each condition. *C*, For detection of phospho-Akt by immunoblot, protein extracts were obtained from cells treated as in *A*, with or without AMD3100 pretreatment. Membrane was probed with anti-phospho-Akt Ab (*upper panel*), stripped, and reprobed with anti-Akt Ab (*lower panel*). The ratio was determined as described in Fig. 2*B*.

dose-dependent increase in F-actin (Fig. 4*A*). The kinetics of SDF-1-induced actin polymerization was rapid, with peak response achieved 15 s poststimulation. Stimulation with gp120 also induced an actin polymerization response, which reached a doubling of F-actin content at 80 nM and was further increased at 200 nM. The kinetics of gp120-induced actin polymerization was slightly delayed, with a peak response achieved 30 s poststimulation. Comparison of peak actin responses from three independent experiments showed that gp120-induced responses at 200 nM were not significantly different from those induced by SDF-1 at 30 nM (Fig. 4*B*). Pretreating cells with AMD3100 or PTX abrogated actin polymerization, indicating a dependence on signaling through CXCR4 and Gαi proteins, respectively (Fig. 4*C*). Pretreatment by SDF-1 rendered $CD4^+$ T cells refractory to gp120-induced actin polymerization (Fig. 4*D*). Because SDF-1 is known to signal solely through CXCR4, these data demonstrated that homologous desensitization of CXCR4 blocked gp120 effects on the cytoskeleton. Complexing gp120 with an excess of sCD4 did not decrease actin polymerization, indicating that signal transduction through cellular CD4 was not required for this response (Fig. 4*E*). Taken together, these findings showed that gp120 and SDF-1 induced cytoskeleton rearrangements through common CXCR4-dependent pathways.

We further analyzed the effects of CXCR4 ligands on cellular morphology and motility by imaging the actin cytoskeleton. Fluorescence imaging of TRITC-phalloidin-labeled cells showed that $CD4^+$ T cells were rounded and harbored a relatively thin layer of cortical actin in the absence of CXCR4 ligands (Fig. 5*A*, *top panels*). Stimulation with SDF-1 and gp120 induced profuse cellular shape changes and the formation of actin-rich protrusions (Fig. 5*A*, *middle* and *lower panels*). Morphological changes were observed in the majority of cells (>75%). The lower percentage of cellular deformations observed in the GFP-Akt-PH experiment (Fig. 3*A*) could be explained by a slight inhibitory effect of the nucleoporation procedure. Quantitative analysis of cellular deformation showed that the shape index was significantly increased after SDF-1 or gp120 stimulation ($p < 0.0001$ for both ligands), indicating that stimulated cells deviated from the circular shape (Fig. 5*B*). Cellular deformations were induced to a similar extent by both ligands and were abrogated by AMD3100 pretreatment (Fig. 5*B* and not shown). The dynamics of cellular deformation were explored by spinning disk confocal imaging, a technique that combines the precision of confocal images with the advantages of live cell analysis. $CD4^+$ T cells nucleoporated with a GFP-actin construct showed vigorous membrane ruffling when pulsed with SDF-1 (Fig. 5*C*, *top panels*, and supplemental movie 1[5]). Cells pulsed with gp120 showed similar deformations, though with a slightly delayed kinetics (Fig. 5*C*, *bottom panels* and movie-2[5]). Membrane ruffling persisted for at least 15 min, indicating that $CD4^+$ T cells remained susceptible to gp120 effects for prolonged periods of time.

We next assessed whether gp120 had the capacity to promote the coordinated rearrangements of the cytoskeleton that lead to directed cell migration. In a Transwell assay, SDF-1 had a detectable effect at 3 nM and caused >60% cell migration at 30 nM (Fig. 6*A*). gp120 also displayed a dose-dependent chemotactic activity on $CD4^+$ T cells, with 34% cell migration at the 200 nM concentration. This activity was abrogated by pretreatment with AMD3100 and PTX, indicating a dependence on signaling through CXCR4 and Gαi proteins, respectively (Fig. 6*B*). Preincubation with sCD4 increased gp120-induced cell migration ($p = 0.04$; Fig. 6*C*), suggesting that sCD4-induced conformational changes promoted gp120 signaling through CXCR4. Thus, gp120 increased cytoskeleton plasticity and functioned as a chemoattractant for primary $CD4^+$ T cells.

Virion-associated gp120 induces actin polymerization and chemotaxis

HIV-1 surface envelope glycoproteins are produced under two forms in infected individuals: monomeric gp120 secreted by productively infected cells and trimeric gp120 present at the surface of virions. Because the conformation of trimeric gp120 is known to differ from that of the monomeric form (50, 51), we investigated whether virion-bound trimeric gp120 could also induce functional responses such as actin polymerization and chemotaxis. We used AT-2-inactivated HIV-1 NL4–3 virions, which harbor intact envelope glycoproteins but are unable to initiate productive infection due to covalent modification of nucleocapsid proteins (35). These inactivated virions are competent for entry, but are blocked in later steps of the viral life cycle, which makes them useful to assess envelope-mediated events (7). AT-2 HIV-1 did trigger actin polymerization in unstimulated $CD4^+$ T cells (Fig. 7*A*). No response was detected if cells were incubated with AMD3100 before stimulation with virions. Importantly, AT-2-inactivated virions devoid of envelope glycoproteins (HIV-1 Δenv) did not give a response

[5] The online version of this article contains supplemental material.

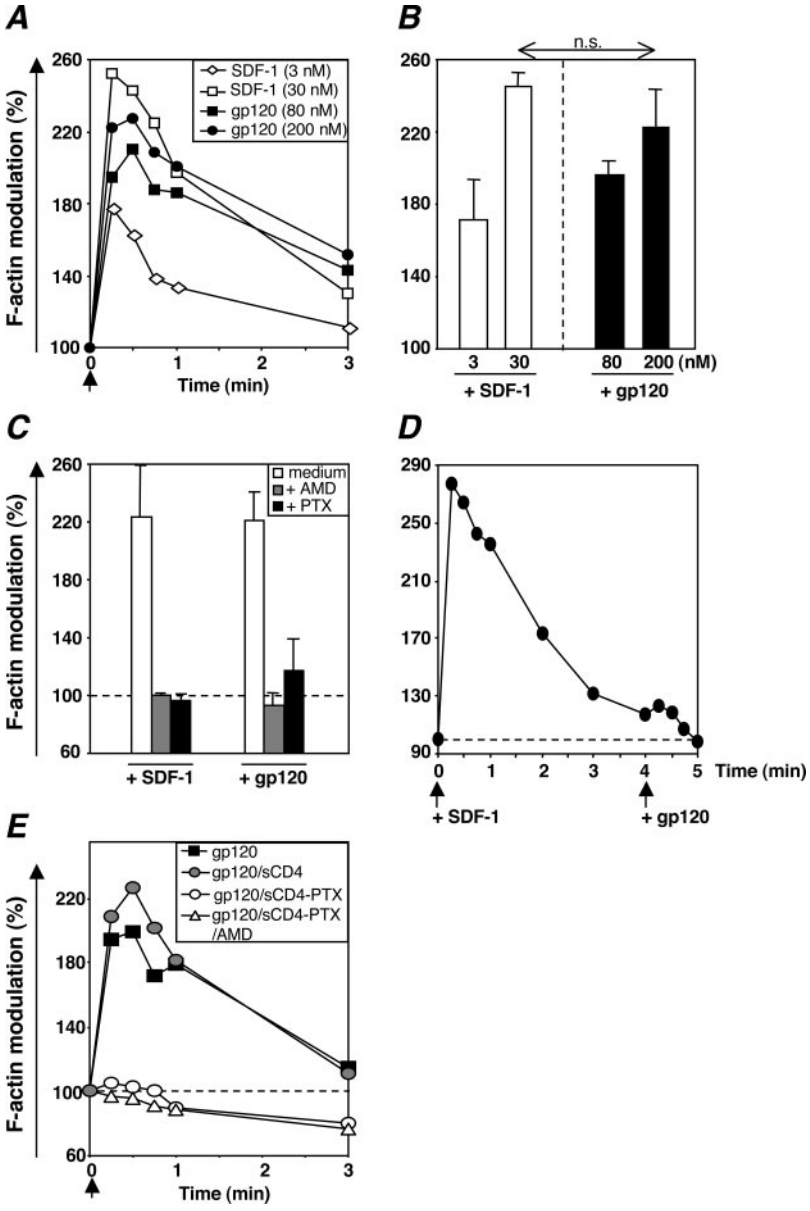

FIGURE 4. gp120 induces actin polymerization in primary $CD4^+$ T lymphocytes. *A*, $CD4^+$ T lymphocytes were tested by flow cytometry for SDF-1- or gp120-triggered actin polymerization using FITC-phalloidin as a probe for intracellular F-actin. Results show the kinetics of actin polymerization following SDF-1 or gp120 stimulation (↑) at the indicated concentrations. 100% corresponds to the baseline level of unstimulated cells. Results are representative of three independent experiments. *B*, The peak actin polymerization values obtained 15 s after stimulation with SDF-1 or 30 s after stimulation with gp120 are compared. Mean values (± SD) from three independent experiments are reported. n.s., not significant. *C*, After treatment with the inhibitors AMD3100 (60 min) or PTX (180 min), $CD4^+$ T cells were stimulated with 30 nM SDF-1 or 200 nM gp120 and analyzed for actin polymerization. Mean peak values (± SD) from three independent experiments are reported. *D*, Desensitization of CXCR4 with SDF-1 inhibits gp120-induced actin polymerization. $CD4^+$ T cells were stimulated with SDF-1 (30 nM) at $t = 0$ and restimulated with gp120 (200 nM) at $t = 4$ min. *E*, Effect of sCD4 on gp120-induced actin response. $CD4^+$ T cells, preincubated or not with PTX alone or in combination with AMD3100, were stimulated with 200 nM gp120 or sCD4/gp120 complexes (↑). Results are representative of three independent experiments.

above baseline. This indicated that HIV gp120, and not one of the multiple cell surface protein spontaneously incorporated into virions, was responsible for the actin polymerization response in a CXCR4-dependent manner. Thus, gp120 in both its monomeric and trimeric forms had the capacity to cause rearrangements of the actin cytoskeleton.

We next tested the capacity of whole HIV-1 virions to induce chemotaxis in a Transwell assay. AT-2 HIV-1 virions promoted $CD4^+$ T cell migration, while AT-2 HIV-1 Δenv did not (Fig. 7*B*). The extent of migration depended on the cell donor and varied between 11 and 51% of input cells. Preincubation of $CD4^+$ T cells with AMD3100 abrogated HIV-induced chemotaxis, indicating a requirement for interaction with CXCR4. Taken together, these findings showed that HIV surface envelope glycoprotein, either in monomeric or in native oligomeric form, induced an array of signals that integrated into a functional chemotactic response.

Discussion

This study provides evidence that HIV-1 activates major CXCR4-dependent signal transduction pathways and acts as a chemoattractant for unstimulated primary $CD4^+$ T cells. Though X4 gp120 was previously reported to activate only a subset of CXCR4-dependent pathways, we found that it could function as a full CXCR4 agonist when used at concentrations that allowed significant occupancy of the receptor. In this context, we demonstrate for the first time that HIV-1 surface envelope glycoprotein gp120 induces the activation of heterotrimeric G proteins. That gp120 induces this very proximal and central event in the CXCR4 signal transduction cascade supports the idea that gp120 signals as a chemokine. In addition, treatment of $CD4^+$ T cells with gp120 also induced rapid calcium mobilization, actin polymerization, and chemotaxis, which are hallmarks of chemokine responses.

gp120 from X4 HIV-1 strains was reported to be defective for the activation of the Erk-1/2 MAPK pathway in unstimulated primary $CD4^+$ T cells, as well as in T cell clones (19, 20). However, gp120 could activate Erk-1/2 in primary $CD4^+$ T cells that had been stimulated through the TCR, suggesting that the activation status of target cells controlled their susceptibility to gp120-induced signals (19). Consistent with other groups, we observed that gp120 used at 80 nM rarely induced detectable phosphorylation of Erk-1/2, while it did cause chemotaxis. In contrast, gp120 tested at 200 nM, a concentration close to its K_d for CXCR4 (47, 48), did

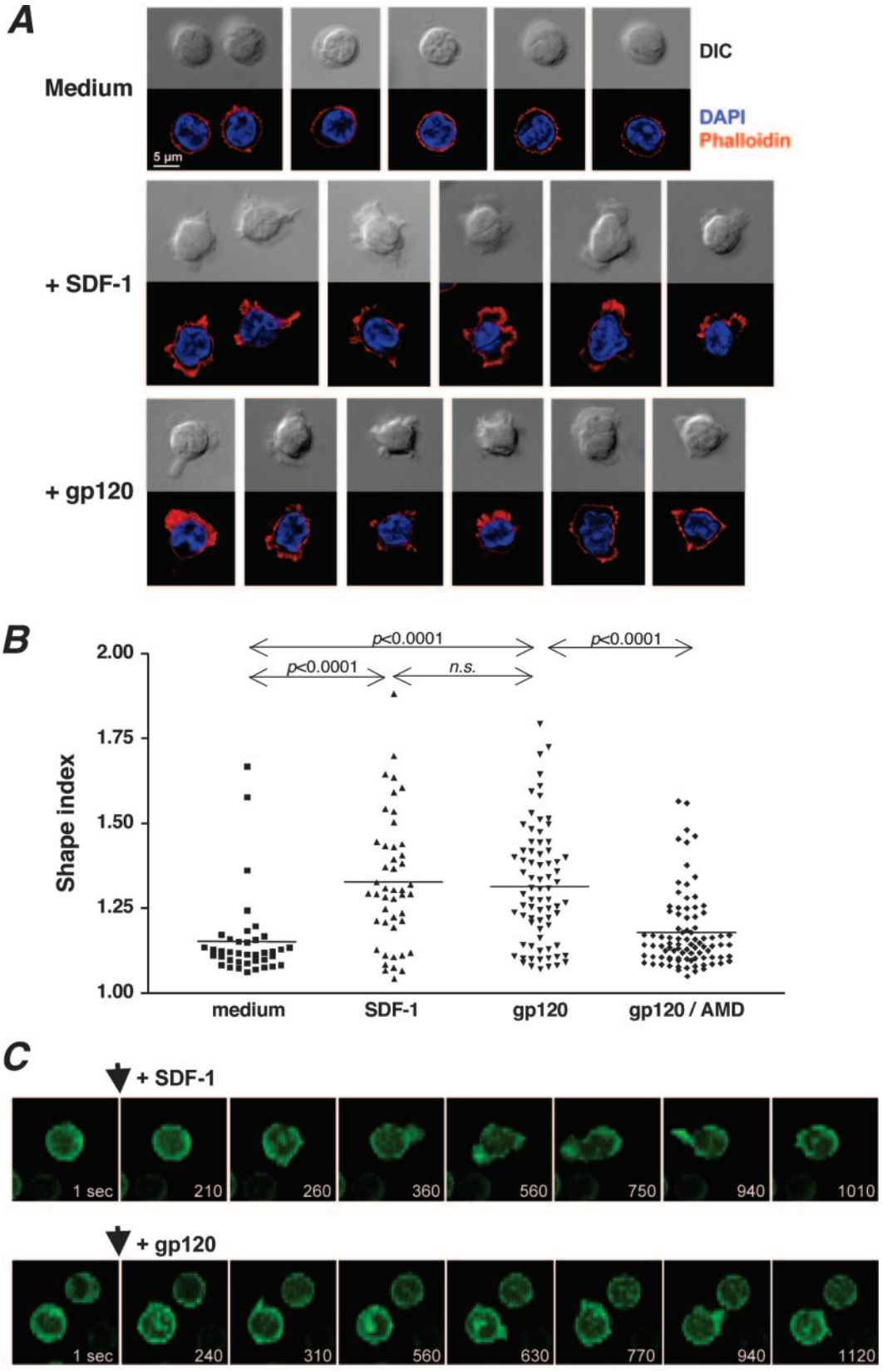

FIGURE 5. gp120 induces actin cytoskeleton rearrangements and dynamic cell deformations in primary $CD4^+$ T lymphocytes. *A*, To visualize the actin cytoskeleton, $CD4^+$ T lymphocytes were stained with TRITC-phalloidin and analyzed by structured illumination microscopy (ApoTome System; Zeiss). For each condition (stimulation with medium alone, SDF-1, or gp120), typical fluorescence and differential interference contrast (DIC) images are shown for six representative cells. Results shown are representative of four independent experiments with >40 cells analyzed per experiment. *B*, Quantitative analysis of SDF-1- or gp120-induced cellular deformations in $CD4^+$ T cells, pretreated or not with AMD3100. Any deviation from a circular shape gives a shape index >1. Lines represent mean values. *C*, Dynamic studies of cytoskeleton rearrangements by spinning-disk confocal analysis. $CD4^+$ T lymphocytes transfected with GFP-actin and plated on glass coverslips were pulsed with SDF-1 or gp120 when indicated (arrows). Images were extracted from movies showing the kinetics of membrane ruffling induced by the two ligands (see data supplement[5]).

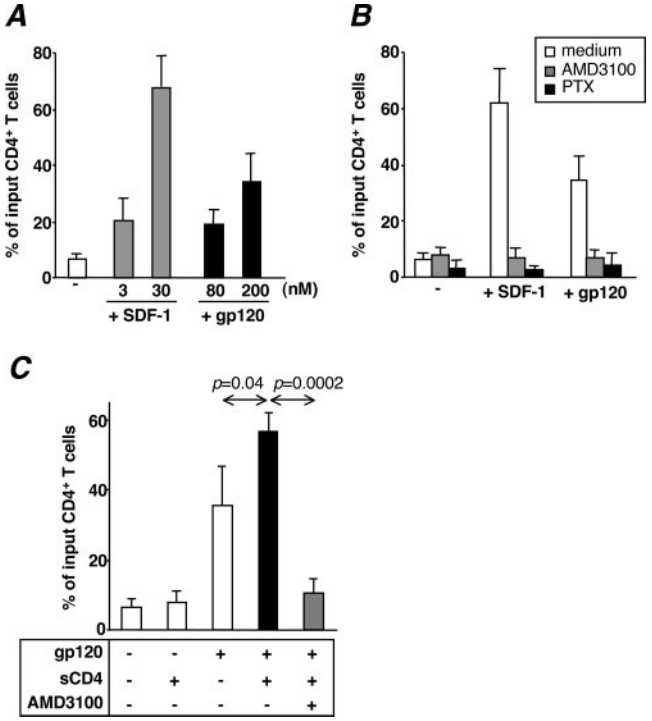

FIGURE 6. gp120 is chemotactic for primary $CD4^+$ T lymphocytes. *A*, Migration of $CD4^+$ T lymphocytes in response to SDF-1 or gp120, at the indicated concentrations, was evaluated using a Transwell assay. The random movement of T cells (chemokinesis) was minimal when equal amounts of ligands (SDF-1 or gp120) were added to the upper and lower chambers (not shown). *B*, After treatment with medium alone, AMD3100, or PTX, $CD4^+$ T cells were tested for chemotaxis in response to SDF-1 or gp120. *C*, $CD4^+$ T cell migration in response to sCD4, gp120, or sCD4/gp120 complexes was evaluated in the presence or absence of AMD3100. *A–C*, Results are expressed as the percentage of input $CD4^+$ T cells that migrated to the lower chamber and represent the mean ± SD of three independent experiments. SDF-1, gp120, sCD4, and sCD4/gp120 complexes were added to the lower chamber only, whereas inhibitors were added to both the upper and lower chambers.

cause Erk-1/2 phosphorylation in unstimulated $CD4^+$ T cells from most donors. This threshold effect suggests that triggering the MAPK pathway requires a higher occupancy of receptors as compared with other pathways. One group reported an absence of MAPK phosphorylation following stimulation with 400 nM gp120 (19). Possible reasons for this discrepancy include the inherent variability in primary cell responses and differences in the sensitivity of the assays. The flow cytometry-based method used in the present study allows the detection of MAPK phosphorylation in a small percentage of cells, which may remain undetectable in the classical immunoblot assay. We also observed that anti-CD3 stimulation reinforced gp120-induced Erk-1/2 phosphorylation (not shown), confirming that stimulation through the TCR lowers the threshold for MAPK activation. Thus, gp120 activated the MAPK cascade in unstimulated as well as activated $CD4^+$ T cells, supporting its role as a full CXCR4 agonist.

The intensity of gp120-induced signaling was comparable or even higher than that induced by the chemokine SDF-1 when compared at concentrations close to their respective K_d (200 and 3 nM) (Fig. 4*B* and 6*A*). However, we chose to perform most assays at 30 nM SDF-1, so as to achieve optimal responses for this chemokine. When compared with 30 nM SDF-1, the signals induced by 200 nM gp120 were generally lower, with the exception of PI3K activation. In the later case, gp120 induced comparable or slightly higher responses than SDF-1 in terms of both GFP-Akt-PH relocalization and Akt phosphorylation (Fig. 3, *B* and *C*). This differential effect would suggest qualitative differences in SDF-1 and gp120-mediated signaling, possibly because gp120 also binds and transduces signals through CD4 (9). How CXCR4- and CD4-dependent pathways intersect requires further investigation.

Of note, X4 gp120 was reported to be defective or less efficient than R5 strains at inducing calcium mobilization in activated $CD4^+$ T cells (22). Because signaling through the TCR inhibits CXCR4-mediated signaling (52), it is possible that prior activation of $CD4^+$ T cells contributes to these differences. Dendritic cells and macrophages are other cell types in which X4 gp120 signals inefficiently and is defective for chemotaxis (23, 25, 31). One contributing factor is limiting CXCR4 expression in immature dendritic cells (53), and possibly in macrophages (54). The incomplete signaling of X4 gp120 in macrophages may account for the limited capacity of X4 HIV-1 strains to replicate in these cells (23). In contrast, we show that X4 strains have the capacity to signal in $CD4^+$ T cells, which may contribute to their abnormal activation and possibly to their infection in late stage disease (11). Generalized activation may thus underlie the precipitous

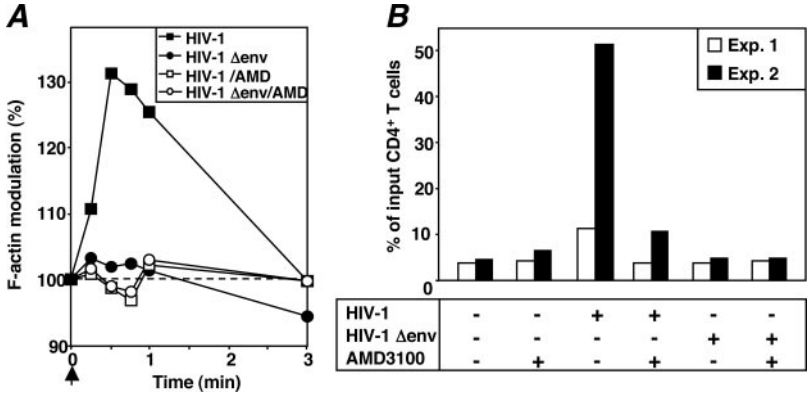

FIGURE 7. Virion-associated gp120 induces actin polymerization and chemotaxis of primary $CD4^+$ T cells. *A*, Actin polymerization response induced by AT-2-inactivated viral particles. $CD4^+$ T lymphocytes, pretreated or not with AMD3100 for 60 min and stimulated with AT-2-inactivated HIV particles, were stained with FITC-phalloidin and analyzed by flow cytometry. Results show the kinetics of actin polymerization following stimulation (↑) with HIV-1 NL4–3 or HIV-1 Δenv (both used at a final concentration of 3 μg p24/ml). Results are representative of three independent experiments. *B*, Virion-induced chemotaxis. After incubation with or without AMD3100 for 60 min, $CD4^+$ T cells were tested for chemotaxis in response to AT-2 HIV-1 virions. Results are shown for independent experiments with two cell donors (Exp.1 and Exp.2) and are expressed as the percentage of input $CD4^+$ T cells that migrated to the lower chamber. Virions were added to the lower chamber at a final concentration of 3 μg of p24 Gag/ml, whereas AMD3100 was added to both the upper and lower chambers.

decline of $CD4^+$ T cells associated with the emergence of X4 strains in patients (33).

Our results show that gp120 has the capacity to perturb the predominant $CD4^+$ $CXCR4^+$ T cell population in lymphoid organs and peripheral blood. Whether gp120 levels reach concentrations sufficient to trigger signaling in vivo has been debated (55). Levels of gp120 in plasma are unlikely to reach the CXCR4 signaling threshold because they are in the picomolar rather than in the nanomolar range (56), well below its K_d value for CXCR4. Complexing of gp120 with circulating Abs further reduces the likelihood of reaching levels required for CXCR4 activation (55). In contrast, $CD4^+$ T cells that traffic in lymphoid organs can be exposed to locally high concentrations of viral glycoproteins. Lymphoid tissues concentrate productively infected cells as well as virions trapped as immune complexes at the surface of follicular dendritic cells (57). The continuous recirculation of naive $CD4^+$ T cells through tightly packed lymphoid tissues is geared toward maximal exposure to foreign Ags and thus will promote interactions with HIV proteins. Productively infected cells in lymphoid tissues express high levels of virus, with a mean of 5,000 HIV-1 genomic RNA copies per cell (58). In addition, the use of sensitive in situ hybridization techniques in the SIV/macaque model has revealed recently that released virions cluster in the periphery of productively infected cells within lymphoid tissues (59). Another source of viral glycoprotein consists in soluble gp120 secreted by infected cells. Because X4 gp120 has the capacity to bind heparan sulfates, secreted gp120 may form gradients at the surface of the extracellular matrix like chemokines do (60). Thus, recirculating T cells that contact productively infected cells will be exposed locally to several concentrated sources of viral glycoprotein, deriving from gp120 expressed at the cell membrane, bound to heparan sulfates, and incorporated at the surface of neighboring virions. The resulting signaling cascades are likely to increase the retention of $CXCR4^+$ cells in the vicinity of viral sources, promoting further interactions with gp120 at the surface of infected cells and virions. The conjunction of high target cell density and high gp120 concentration in lymphoid organs likely contributes to make these organs preferential sites of viral spread and T cell dysregulation. In contrast, sites that express constitutively high levels of the chemokine SDF-1, such as the gut mucosa, may be protected against the immunopathogenic effects of X4 viruses (61).

It is relevant that virion-associated gp120, and not only soluble gp120, caused cytoskeleton rearrangements and chemotaxis. We used AT-2 HIV-1 viral preparations at a concentration of 3 μg/ml Gag p24 Ag, which corresponds to an estimated gp120 concentration of 2 nM, given a Gag to gp120 ratio of $\sim$60 (62). These data suggest that virion-associated gp120 can signal in the nanomolar range. Because soluble gp120 induced low or undetectable chemotactic responses at 2 nM (not shown), virion-associated gp120 may actually be more efficient at signaling through CXCR4 than soluble gp120. The particulate or trimeric nature of virion-bound gp120 may increase the avidity of the interaction with CXCR4 and possibly enhance signaling through cross-linking of the chemoreceptor. Therefore, virions could play a significant role in the altered trafficking and activation patterns of $CD4^+$ T cells.

The capacity of gp120 to induce cytoskeleton rearrangements was unambiguously revealed by real-time video-microscopy as well as quantitative measurements of actin polymerization. It was striking that gp120 proved as potent as the chemokine SDF-1 in inducing rapid membrane ruffling and formation of actin-rich protrusions. These observations immediately suggest mechanisms that could promote HIV-1 entry and dissemination. Surrounding of viral particles by membrane protrusions increases the virus/cell interaction surface, which may facilitates viral capture. Active rearrangements of the cytoskeleton may help viral particles to cross the barrier of cortical actin in newly infected cells. Indeed, viruses such as HIV that enter target cells by fusion at the plasma membrane are at a disadvantage compared with viruses that use the endocytic route and are delivered deep within the cytoplasm (63). It may be to overcome the obstacle of cortical actin that several of HIV proteins, including gp120 and Nef, acquired the capacity to control actin dynamics (64). Actin rearrangements also have consequences on HIV transfer from cell to cell. Expression of HIV envelope glycoprotein at the cell surface was recently shown to cause the formation of a "virological synapse" with neighboring $CD4^+$ $CXCR4^+$ cells (65). Formation of this actin-dependent junction facilitated the cell to cell transfer of HIV particles. Our findings help understand how such a structure may form. The high concentration of gp120 present at the surface of productively infected cells is bound to activate CXCR4-dependent signal transduction pathways in adjoining cells, which will cause cytoskeleton rearrangements polarized toward the source of viral proteins, and thus initiate cellular junctions.

Recent evidence indicate that resting T cells from HIV-1-infected patients are not truly resting but rather suboptimally activated. It is relevant, for instance, that resting $CD4^+$ T cells from patients that remain viremic despite therapy spontaneously produce HIV particles (66). DNA micro- and macroarray analysis revealed perturbed transcriptional patterns in patient T lymphocytes, with increased expression of several gene families involved in T cell activation (66, 67). This suggests that resting $CD4^+$ T cells from patients reach a preactivated state that allows some degree of viral production. Our findings support the idea that gp120-induced signals transduced through CXCR4 could contribute to the abnormal activation status of resting $CD4^+$ T cells. Whether these signals are sufficient to promote viral replication warrants further investigation.

In conclusion, HIV has the capacity to exploit CXCR4-dependent transduction pathways at multiple levels. By functioning as a chemokine, gp120 may 1) recruit and/or retain target cells close to sources of virus, 2) trigger cytoskeleton rearrangements that facilitate viral entry, 3) preactivate resting $CD4^+$ T cells, possibly making them competent for viral replication, and 4) perturb the trafficking and responses of the vast majority of $CD4^+$ T cells that express CXCR4, including resting T cells. Blocking these aberrant signals may lead to novel immunotherapeutic approaches to AIDS treatment.

Acknowledgments

We thank Emmanuelle Perret and Pascal Roux for help with imaging, Marie-Christine Wagner for help with calcium flux analysis, Georges Bismuth for providing advice and reagents, Tobias Meyer for providing the GFP-Akt-PH plasmid, and Cecilia Cheng-Mayer and Dominique Emilie for critical reading of the manuscript.

References

1. Feng, Y., C. C. Broder, P. E. Kennedy, and E. A. Berger. 1996. HIV-1 entry cofactor: Functional cDNA cloning of a seven-transmembrane, G protein-coupled receptor. *Science 272:872*.
2. Wyatt, R., and J. Sodroski. 1998. The HIV-1 envelope glycoproteins: fusogens, antigens, and immunogens. *Science 280:1884*.
3. Moore, J. P., S. G. Kitchen, P. Pugach, and J. A. Zack. 2004. The CCR5 and CXCR4 coreceptors—central to understanding the transmission and pathogenesis of human immunodeficiency virus type 1 infection. *AIDS Res. Hum. Retroviruses 20:111*.
4. Marschner, S., T. Hunig, J. C. Cambier, and T. H. Finkel. 2002. Ligation of human CD4 interferes with antigen-induced activation of primary T cells. *Immunol. Lett. 82:131*.
5. Chirmule, N., and S. Pahwa. 1996. Envelope glycoproteins of human immunodeficiency virus type 1: Profound influences on immune functions. *Microbiol. Rev. 60:386*.

6. Zhang, R., C. J. Fichtenbaum, D. A. Hildeman, J. D. Lifson, and C. Chougnet. 2004. CD40 ligand dysregulation in HIV infection: HIV glycoprotein 120 inhibits signaling cascades upstream of CD40 ligand transcription. *J. Immunol. 172:2678*.
7. Esser, M. T., J. W. Bess, Jr., K. Suryanarayana, E. Chertova, D. Marti, M. Carrington, L. O. Arthur, and J. D. Lifson. 2001. Partial activation and induction of apoptosis in $CD4^+$ and $CD8^+$ T lymphocytes by conformationally authentic noninfectious human immunodeficiency virus type 1. *J. Virol. 75:1152*.
8. Kinter, A., J. Arthos, C. Cicala, and A. S. Fauci. 2000. Chemokines, cytokines and HIV: A complex network of interactions that influence HIV pathogenesis. *Immunol. Rev. 177:88*.
9. Stantchev, T. S., and C. C. Broder. 2001. Human immunodeficiency virus type-1 and chemokines: Beyond competition for common cellular receptors. *Cytokine Growth Factor Rev. 12:219*.
10. Grossman, Z., M. Meier-Schellersheim, A. E. Sousa, R. M. Victorino, and W. E. Paul. 2002. $CD4^+$ T-cell depletion in HIV infection: Are we closer to understanding the cause? *Nat. Med. 8:319*.
11. Hazenberg, M. D., D. Hamann, H. Schuitemaker, and F. Miedema. 2000. T cell depletion in HIV-1 infection: How $CD4^+$ T cells go out of stock. *Nat. Immunol. 1:285*.
12. Douek, D. C., L. J. Picker, and R. A. Koup. 2003. T cell dynamics in HIV-1 infection. *Annu. Rev. Immunol. 21:265*.
13. Thelen, M. 2001. Dancing to the tune of chemokines. *Nat. Immunol. 2:129*.
14. Moser, B., M. Wolf, A. Walz, and P. Loetscher. 2004. Chemokines: Multiple levels of leukocyte migration control. *Trends Immunol. 25:75*.
15. Shenoy, S. K., and R. J. Lefkowitz. 2003. Multifaceted roles of β-arrestins in the regulation of seven-membrane-spanning receptor trafficking and signalling. *Biochem. J. 375:503*.
16. Wang, F., P. Herzmark, O. D. Weiner, S. Srinivasan, G. Servant, and H. R. Bourne. 2002. Lipid products of PI3Ks maintain persistent cell polarity and directed motility in neutrophils. *Nat. Cell Biol. 4:513*.
17. Davis, C. B., I. Dikic, D. Unutmaz, C. M. Hill, J. Arthos, M. A. Siani, D. A. Thompson, J. Schlessinger, and D. R. Littman. 1997. Signal transduction due to HIV-1 envelope interactions with chemokine receptors CXCR4 or CCR5. *J. Exp. Med. 186:1793*.
18. Francois, F., and M. E. Klotman. 2003. Phosphatidylinositol 3-kinase regulates human immunodeficiency virus type 1 replication following viral entry in primary $CD4^+$ T lymphocytes and macrophages. *J. Virol. 77:2539*.
19. Kinet, S., F. Bernard, C. Mongellaz, M. Perreau, F. D. Goldman, and N. Taylor. 2002. gp120-mediated induction of the MAPK cascade is dependent on the activation state of $CD4^+$ lymphocytes. *Blood 100:2546*.
20. Misse, D., M. Cerutti, N. Noraz, P. Jourdan, J. Favero, G. Devauchelle, H. Yssel, N. Taylor, and F. Veas. 1999. A CD4-independent interaction of human immunodeficiency virus-1 gp120 with CXCR4 induces their cointernalization, cell signaling, and T-cell chemotaxis. *Blood 93:2454*.
21. Popik, W., J. E. Hesselgesser, and P. M. Pitha. 1998. Binding of human immunodeficiency virus type 1 to CD4 and CXCR4 receptors differentially regulates expression of inflammatory genes and activates the MEK/ERK signaling pathway. *J. Virol. 72:6406*.
22. Weissman, D., R. L. Rabin, J. Arthos, A. Rubbert, M. Dybul, R. Swofford, S. Venkatesan, J. M. Farber, and A. S. Fauci. 1997. Macrophage-tropic HIV and SIV envelope proteins induce a signal through the CCR5 chemokine receptor. *Nature 389:981*.
23. Arthos, J., A. Rubbert, R. L. Rabin, C. Cicala, E. Machado, K. Wildt, M. Hanbach, T. D. Steenbeke, R. Swofford, J. M. Farber, and A. S. Fauci. 2000. CCR5 signal transduction in macrophages by human immunodeficiency virus and simian immunodeficiency virus envelopes. *J. Virol. 74:6418*.
24. Liu, Q. H., D. A. Williams, C. McManus, F. Baribaud, R. W. Doms, D. Schols, E. De Clercq, M. I. Kotlikoff, R. G. Collman, and B. D. Freedman. 2000. HIV-1 gp120 and chemokines activate ion channels in primary macrophages through CCR5 and CXCR4 stimulation. *Proc. Natl. Acad. Sci. USA 97:4832*.
25. Lin, C. L., A. K. Sewell, G. F. Gao, K. T. Whelan, R. E. Phillips, and J. M. Austyn. 2000. Macrophage-tropic HIV induces and exploits dendritic cell chemotaxis. *J. Exp. Med. 192:587*.
26. Iyengar, S., D. H. Schwartz, and J. E. Hildreth. 1999. T cell-tropic HIV gp120 mediates CD4 and CD8 cell chemotaxis through CXCR4 independent of CD4: implications for HIV pathogenesis. *J. Immunol. 162:6263*.
27. Brainard, D. M., W. G. Tharp, E. Granado, N. Miller, A. K. Trocha, X. H. Ren, B. Conrad, E. F. Terwilliger, R. Wyatt, B. D. Walker, and M. C. Poznansky. 2004. Migration of antigen-specific T cells away from CXCR4-binding human immunodeficiency virus type 1 gp120. *J. Virol. 78:5184*.
28. Wang, J. S., S. Marschner, and T. H. Finkel. 2004. CXCR4 engagement is required for HIV-1-induced L-selectin shedding. *Blood 103:1218*.
29. Clayton, F., D. P. Kotler, S. K. Kuwada, T. Morgan, C. Stepan, J. Kuang, J. Le, and J. Fantini. 2001. Gp120-induced Bob/GPR15 activation: a possible cause of human immunodeficiency virus enteropathy. *Am. J. Pathol. 159:1933*.
30. Tilton, B., L. Ho, E. Oberlin, P. Loetscher, F. Baleux, I. Clark-Lewis, and M. Thelen. 2000. Signal transduction by CXC chemokine receptor 4. Stromal cell-derived factor 1 stimulates prolonged protein kinase B and extracellular signal-regulated kinase 2 activation in T lymphocytes. *J. Exp. Med. 192:313*.
31. Lee, C., Q. H. Liu, B. Tomkowicz, Y. Yi, B. D. Freedman, and R. G. Collman. 2003. Macrophage activation through CCR5- and CXCR4-mediated gp120-elicited signaling pathways. *J. Leukocyte Biol. 74:676*.
32. Bleul, C. C., L. Wu, J. A. Hoxie, T. A. Springer, and C. R. Mackay. 1997. The HIV coreceptors CXCR4 and CCR5 are differentially expressed and regulated on human T lymphocytes. *Proc. Natl. Acad. Sci. USA 94:1925*.
33. Connor, R. I., K. E. Sheridan, D. Ceradini, S. Choe, and N. R. Landau. 1997. Change in coreceptor use correlates with disease progression in HIV-1-infected individuals. *J. Exp. Med. 185:621*.
34. Amara, A., O. Lorthioir, A. Valenzuela, A. Magerus, M. Thelen, M. Montes, J. L. Virelizier, M. Delepierre, F. Baleux, H. Lortat-Jacob, and F. Arenzana-Seisdedos. 1999. Stromal cell-derived factor-1α associates with heparan sulfates through the first β-strand of the chemokine. *J. Biol. Chem. 274:23916*.
35. Arthur, L. O., J. W. Bess, Jr., E. N. Chertova, J. L. Rossio, M. T. Esser, R. E. Benveniste, L. E. Henderson, and J. D. Lifson. 1998. Chemical inactivation of retroviral infectivity by targeting nucleocapsid protein zinc fingers: A candidate SIV vaccine. *AIDS Res. Hum. Retroviruses 14 Suppl. 3:S311*.
36. Mullins, J. I. Accessed 2004. Gradient purification of AT2-inactivated HIV-1. ubik.microbiol.washington.edu/protocols/bl3/at2.htm.
37. Blanpain, C., J. M. Vanderwinden, J. Cihak, V. Wittamer, E. Le Poul, H. Issafras, M. Stangassinger, G. Vassart, S. Marullo, D. Schlndorff, M. Parmentier, and M. Mack. 2002. Multiple active states and oligomerization of CCR5 revealed by functional properties of monoclonal antibodies. *Mol. Biol. Cell. 13:723*.
38. Rabin, R. L., M. K. Park, F. Liao, R. Swofford, D. Stephany, and J. M. Farber. 1999. Chemokine receptor responses on T cells are achieved through regulation of both receptor expression and signaling. *J. Immunol. 162:3840*.
39. Chakrabarti, L. A., S. R. Lewin, L. Zhang, A. Gettie, A. Luckay, L. N. Martin, E. Skulsky, D. D. Ho, C. Cheng-Mayer, and P. A. Marx. 2000. Normal T-cell turnover in sooty mangabeys harboring active simian immunodeficiency virus infection. *J. Virol. 74:1209*.
40. Harriague, J., P. Debré, G. Bismuth, and P. Hubert. 2000. Priming of CD2-induced p62Dok tyrosine phosphorylation by CD3 in Jurkat T cells. *Eur. J. Immunol. 30:3319*.
41. Balabanian, K., A. Foussat, P. Dorfmuller, I. Durand-Gasselin, F. Capel, L. Bouchet-Delbos, A. Portier, A. Marfaing-Koka, R. Krzysiek, A. C. Rimaniol, G. Simonneau, D. Emilie, and M. Humbert. 2002. CX3C chemokine fractalkine in pulmonary arterial hypertension. *Am. J. Respir. Crit. Care Med. 165:1419*.
42. Balabanian, K., A. Foussat, L. Bouchet-Delbos, J. Couderc, R. Krzysiek, A. Amara, F. Baleux, A. Portier, P. Galanaud, and D. Emilie. 2002. Interleukin-10 modulates the sensitivity of peritoneal B lymphocytes to chemokines with opposite effects on stromal cell-derived factor-1 and B-lymphocyte chemoattractant. *Blood 99:427*.
43. Haugh, J. M., F. Codazzi, M. Teruel, and T. Meyer. 2000. Spatial sensing in fibroblasts mediated by 3′ phosphoinositides. *J. Cell Biol. 151:1269*.
44. Neil, M. A. A., R. Juskaitis, and T. Wilson. 1997. Method of obtaining optical sectioning by using structured light in a conventional microscope. *Opt. Lett. 22:1905*.
45. Harriague, J., and G. Bismuth. 2002. Imaging antigen-induced PI3K activation in T cells. *Nat. Immunol. 3:1090*.
46. Arrieumerlou, C., E. Donnadieu, P. Brennan, G. Keryer, G. Bismuth, D. Cantrell, and A. Trautmann. 1998. Involvement of phosphoinositide 3-kinase and Rac in membrane ruffling induced by IL-2 in T cells. *Eur. J. Immunol. 28:1877*.
47. Babcock, G. J., T. Mirzabekov, W. Wojtowicz, and J. Sodroski. 2001. Ligand binding characteristics of CXCR4 incorporated into paramagnetic proteoliposomes. *J. Biol. Chem. 276:38433*.
48. Hoffman, T. L., G. Canziani, L. Jia, J. Rucker, and R. W. Doms. 2000. A biosensor assay for studying ligand-membrane receptor interactions: Binding of antibodies and HIV-1 Env to chemokine receptors. *Proc. Natl. Acad. Sci. USA 97:11215*.
49. Trkola, A., T. Dragic, J. Arthos, J. M. Binley, W. C. Olson, G. P. Allaway, C. Cheng-Mayer, J. Robinson, P. J. Maddon, and J. P. Moore. 1996. CD4-dependent, antibody-sensitive interactions between HIV-1 and its co-receptor CCR-5. *Nature 384:184*.
50. Ugolini, S., I. Mondor, and Q. J. Sattentau. 1999. HIV-1 attachment: Another look. *Trends Microbiol. 7:144*.
51. Fouts, T. R., J. M. Binley, A. Trkola, J. E. Robinson, and J. P. Moore. 1997. Neutralization of the human immunodeficiency virus type 1 primary isolate JR-FL by human monoclonal antibodies correlates with antibody binding to the oligomeric form of the envelope glycoprotein complex. *J. Virol. 71:2779*.
52. Peacock, J. W. and F. R. Jirik. 1999. TCR activation inhibits chemotaxis toward stromal cell-derived factor-1: Evidence for reciprocal regulation between CXCR4 and the TCR. *J. Immunol. 162:215*.
53. Canque, B., Y. Bakri, S. Camus, M. Yagello, A. Benjouad, and J. C. Gluckman. 1999. The susceptibility to X4 and R5 human immunodeficiency virus-1 strains of dendritic cells derived in vitro from $CD34^+$ hematopoietic progenitor cells is primarily determined by their maturation stage. *Blood 93:3866*.
54. Tokunaga, K., M. L. Greenberg, M. A. Morse, R. I. Cumming, H. K. Lyerly, and B. R. Cullen. 2001. Molecular basis for cell tropism of CXCR4-dependent human immunodeficiency virus type 1 isolates. *J. Virol. 75:6776*.
55. Klasse, P. J., and J. P. Moore. 2004. Is there enough gp120 in the body fluids of HIV-1-infected individuals to have biologically significant effects? *Virology 323:1*.
56. Gilbert, M., J. Kirihara, and J. Mills. 1991. Enzyme-linked immunoassay for human immunodeficiency virus type 1 envelope glycoprotein 120. *J. Clin. Microbiol. 29:142*.
57. Pantaleo, G., C. Graziosi, J. F. Demarest, L. Butini, M. Montroni, C. H. Fox, J. M. Orenstein, D. P. Kotler, and A. S. Fauci. 1993. HIV infection is active and progressive in lymphoid tissue during the clinically latent stage of disease. *Nature 362:355*.
58. Hockett, R. D., J. M. Kilby, C. A. Derdeyn, M. S. Saag, M. Sillers, K. Squires, S. Chiz, M. A. Nowak, G. M. Shaw, and R. P. Bucy. 1999. Constant mean viral

copy number per infected cell in tissues regardless of high, low, or undetectable plasma HIV RNA. *J. Exp. Med. 189:1545*.

59. Zhang, Z. Q., S. W. Wietgrefe, Q. Li, M. D. Shore, L. Duan, C. Reilly, J. D. Lifson, and A. T. Haase. 2004. Roles of substrate availability and infection of resting and activated $CD4^+$ T cells in transmission and acute simian immunodeficiency virus infection. *Proc. Natl. Acad. Sci. USA 101:5640*.
60. Moulard, M., H. Lortat-Jacob, I. Mondor, G. Roca, R. Wyatt, J. Sodroski, L. Zhao, W. Olson, P. D. Kwong, and Q. J. Sattentau. 2000. Selective interactions of polyanions with basic surfaces on human immunodeficiency virus type 1 gp120. *J. Virol. 74:1948*.
61. Agace, W. W., A. Amara, A. I. Roberts, J. L. Pablos, S. Thelen, M. Uguccioni, X. Y. Li, J. Marsal, F. Arenzana-Seisdedos, T. Delaunay, E. C. Ebert, B. Moser, and C. M. Parker. 2000. Constitutive expression of stromal derived factor-1 by mucosal epithelia and its role in HIV transmission and propagation. *Curr. Biol. 10:325*.
62. Chertova, E., J. W. Bess Jr., Jr., B. J. Crise, I. R. Sowder, T. M. Schaden, J. M. Hilburn, J. A. Hoxie, R. E. Benveniste, J. D. Lifson, L. E. Henderson, and L. O. Arthur. 2002. Envelope glycoprotein incorporation, not shedding of surface envelope glycoprotein (gp120/SU): Is the primary determinant of SU content of purified human immunodeficiency virus type 1 and simian immunodeficiency virus. *J. Virol. 76:5315*.
63. Smith, A. E., and A. Helenius. 2004. How viruses enter animal cells. *Science 304:237*.
64. Campbell, E. M., R. Nunez, and T. J. Hope. 2004. Disruption of the actin cytoskeleton can complement the ability of nef to enhance human immunodeficiency virus type 1 infectivity. *J. Virol. 78:5745*.
65. Jolly, C., K. Kashefi, M. Hollinshead, and Q. J. Sattentau. 2004. HIV-1 cell to cell transfer across an Env-induced, actin-dependent synapse. *J. Exp. Med. 199:283*.
66. Chun, T. W., J. S. Justement, R. A. Lempicki, J. Yang, G. Dennis, Jr., C. W. Hallahan, C. Sanford, P. Pandya, S. Liu, M. McLaughlin, L. A. Ehler, S. Moir, and A. S. Fauci. 2003. Gene expression and viral prodution in latently infected, resting $CD4^+$ T cells in viremic versus aviremic HIV-infected individuals. *Proc. Natl. Acad. Sci. USA 100:1908*.
67. Johansson, C. C., T. Bryn, A. Yndestad, H. G. Eiken, V. Bjerkeli, S. S. Froland, P. Aukrust, and K. Tasken. 2004. Cytokine networks are pre-activated in T cells from HIV-infected patients on HAART and are under the control of cAMP. *AIDS 18:171*.